Astron. Astrophys. 330, 1109–1119 (1998)

ASTRONOMY AND ASTROPHYSICS

Near-infrared narrow-band photometry of M-giant and Mira stars: models meet observations

R. Alvarez[1] **and B. Plez**[2,3]

[1] GRAAL, Université Montpellier II, UPRESA 5024/CNRS, F-34095 Montpellier Cedex 05, France
[2] Astronomiska Observatoriet, box 515, S-751 20 Uppsala, Sweden
[3] Atomspektroskopi, Fysiska Institution, box 118, S-221 00 Lund, Sweden (plez@fysik.lu.se)

Received 20 June 1997 / Accepted 19 September 1997

Abstract. From near-infrared, narrow-band photometry of 256 oxygen-rich Mira variables we obtain evidence about the loops that these stars follow in colour-colour diagrams. We also find a phase lag between indices related to molecular band-strength of titanium oxide and vanadium oxide. We compute colours for normal M-giants and Miras using hydrostatic and hydrodynamic model atmospheres and very extensive up-to-date line lists. Normal M-giants colours are well reproduced, reaching a high quantitative agreement with observations for spectral types earlier than M7. The out-of-phase variations of the various spectral features of Miras are also acceptably reproduced, despite limitations in the modelling. This enables us to confirm that the phase lag phenomenon results from the propagation of perturbations in the extended atmosphere. It opens new perspectives in the spectral modelling of Miras.

Key words: physical data and processes: molecular data – stars: atmospheres – stars: AGB and post-AGB – stars: variables: Miras

1. Introduction

Red giants and long-period variables provide crucial information on stellar and galactic evolution. It is thus essential to be able to interpret their spectra and photometry in terms of stellar parameters (effective temperature, chemical composition, mass, etc) and physical processes (presence of shocks, of a wind, etc). In spite of the difficulty to model these stars due to the many complications arising from low temperatures (molecule and dust formation) and the often very extended atmosphere, important progress in the modelling of static (Plez et al. 1992; see also the review by Plez 1997) and dynamic (Bowen 1988; Fleischer et al. 1992; Höfner & Dorfi 1997) cool star atmospheres have been achieved in the last years.

Send offprint requests to: alvarez@graal.univ-montp2.fr

Confrontation with observations is the natural aim of any modelling attempt. Checking the validity of the various models' assumptions and inputs is obviously essential. Some recent investigations have dealt with high resolution spectroscopic observations (e.g. Plez et al. 1993) while others concentrated on photometry (Bessell et al. 1996). They demonstrate that model atmospheres and synthetic spectra are now reaching a high quantitative agreement with observations, due to the recent great improvement in opacity completeness and accuracy.

The near-infrared narrow-band photometry of Lockwood (1972), described in Sect. 2, has various qualities which make it very suitable for the study of M-giants and Mira variables. It consists of narrow-band filters around 1 μm, a spectral region where very cool stars emit most of their energy and where, unfortunately, very few observed spectra are available. The narrow-band filters used allow a precise study of absorption features of molecules dominating the optical spectrum of cool stars, titanium oxide (TiO) and vanadium oxide (VO), for which new data have been recently published. Furthermore, Lockwood's data represent one of the very few set of regular observations on whole cycles of a large number of Miras. The study of the effects of pulsation on absorption features is thus possible. Observational evidence for a phase lag between indices related to TiO and VO absortion features is given (Sect. 3). In Sect. 4, synthetic colours from static models are computed and compared to M-giant colours. Thanks to the updated millions of spectral lines taken into account, a remarkable agreement is obtained. In Sect. 5 we compute LTE radiative transfer in hydrodynamic models that satisfactorily reproduce the colour variations and the phase lag for Mira variables.

2. The data

2.1. Lockwood's photometric system

Lockwood (1972; hereafter L72) observed 292 M- and S-type Mira variables from 1969 to 1971 at the Kitt Peak National Observatory, with a five-colour narrow-band photometric system based on Wing's 27 colours system (Wing 1967). He obtained

Table 1. Properties of Lockwood's (1972) five-colour system

Filter designation	Peak wavelength	Half-power bandwidth	Feature (Lockwood 1972)
78	7818 Å	90 Å	TiO
87	8777 Å	82 Å	Continuum (+TiO)
88	8884 Å	114 Å	TiO
104	10351 Å	125 Å	Continuum
105	10506 Å	100 Å	VO

1795 individual sets of five-colour measurements, at different phases, and, for some stars, during several cycles. The narrow-bands were chosen to measure depths of molecular band heads of TiO and VO, or regions relatively free of molecular absorption. Table 1 lists the properties of the five-colour system. The 78 and 88 filters were used to measure several bands of TiO. The VO absorption was measured by the 105 filter. The 87 and 104 filters were expected to match 'continuum' regions. However, it appeared to Lockwood that the 87 filter becomes contaminated by TiO bands in the later M stars. In L72 are tabulated the measurements of the 104 magnitudes and of the four colours: 78−87, 88−87, 87−104, and 105−104. The median standard errors were 0.012 mag for 104 and 0.006 mag for the colours.

Due to the regularity of the observations, this set of data allows a precise study of the behaviour of TiO and VO absorption with phase. For homogeneity reasons, only the oxygen-rich Miras have been subsequently considered. They represent a sample of 256 stars for which 1501 sets of five-colour measurements were obtained at several phases. The period distribution of the sample corresponds perfectly to the one obtained for the M-Miras listed in the General Catalogue of Variable Stars (GCVS; Kholopov 1985, 1987). The stars were observed preferably near maximum and minimum of light curves.

2.2. Molecular band-strength indices

In order to study the behaviour of TiO and VO absorption features with phase, we have considered four indices:

78−88: this index is proportional to the ratio between two different band heads of TiO. It is a good effective temperature indicator for temperatures above 3000 K and thus was prefered to 88−87 originally given in L72. For lower temperatures, the TiO bands begin to saturate.

78−87: the 87 and 88 filters overlap slightly. As a consequence, the 78−88 and 78−87 indices are very similar. The absolute differences are always less than 0.2 mag.

87−104: Lockwood originally hoped to obtain a colour temperature determination from this index as both filters were thought to measure regions free of strong molecular absorption. But filter 87 proves to be contaminated at least by TiO bands.

105−104: it is related to VO bands. This index depends strongly on effective temperature below 3000 K where the VO molecular bands begin to appear.

The first three indices can be considered to measure mainly TiO features (although we will show below that VO bands are also present in these passbands) and 105−104 may be seen as a pure VO index. The indices 78−88 and 105−104 complement each other very well as temperature indicators. They have been used to determine effective temperature for a large number of Miras (Alvarez & Mennessier 1997). The four colours are each defined so as to increase linearly with decreasing effective temperature during a cycle.

3. Variations of TiO and VO absorption features during a cycle. Observational evidence for phase lag

3.1. Phase-colour diagrams

The phases of all sets of measurements are given in L72. They were determined from the mean periods given in the GCVS and the AAVSO annual predictions. Phase zero marks the maximum of the visual light curve. Fig. 1 shows the four indices calculated from the entire data (1501 measurements) plotted against the phase. The curves represent the running average computed for 100 points on a 1/16th cycle interval. The data in the phase interval [0.5 ; 1.0] are reproduced in the interval [-0.5 ; 0.0]. Arrows indicate the extremes of each curve.

Such a plot has of course no real physical significance since the data are composed of observations of 256 different Miras, which exhibit a large spread of periods and mean spectral types. Nevertheless, it gives interesting insights into the global behaviour of the indices with phase. As expected, the colours reach a minimum around phase zero when the effective temperature is highest and reach a maximum around phase 0.5, at minimum light.

The important feature is the phase lag that exists between the 105−104 index and the other indices. The VO index has its minimum value at phase $\varphi = 0.1$ or so, whereas the indices 78−88, 78−87, 87−104 have their minimum slightly before phase zero. The same phase shift of about 0.1 is also found between the maxima: it occurs at $\varphi = 0.6$ for 105−104, and around $\varphi = 0.5$ for the other colours. Note that the dispersion around the mean value is minimum near phase zero for 87−104 and 105−104 and maximum near phase 0.5, whereas the opposite is true of the two other indices. This is explained by the sensitivity, or the lack thereof, of the various indices in the effective temperature range above or below 3000 K (see Fig. 7). As a consequence, the positions of the maxima of the TiO indices (78−87, 78−88) which saturate around 1.8, are not easy to locate accurately. The VO index (105−104) has values clearly greater than zero only near the minimum light. Thus, the presence or not of a phase lag is not totally obvious in Fig. 1. Colour-colour diagrams enable us to confirm that feature.

3.2. Colour-colour diagrams

Figs. 2 and 3 display the average colour-colour variation with phase for 78−88/105−104, and 78−87/87−104 respectively. The average curves of Fig. 1 are simply reported in those colour-

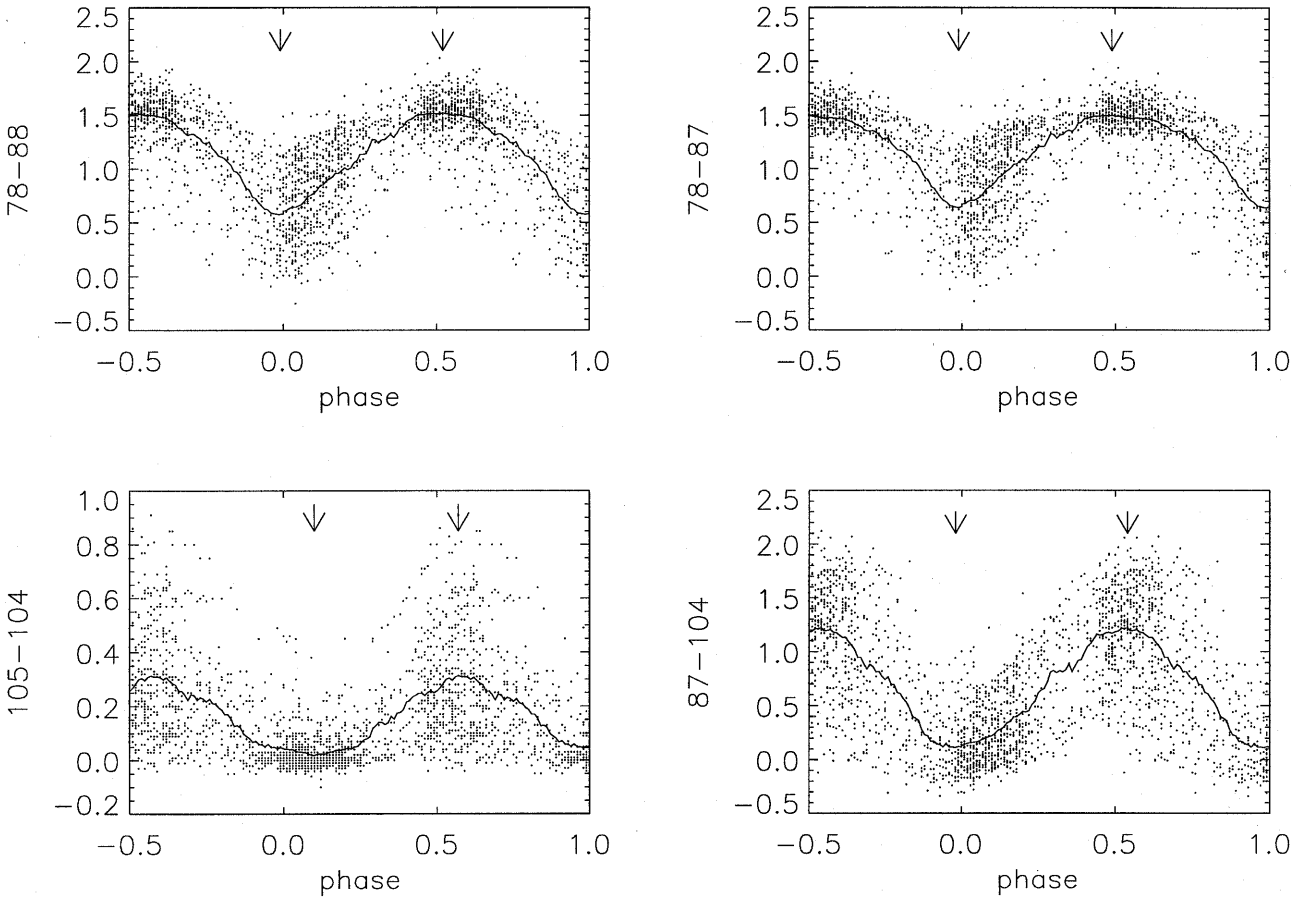

Fig. 1. The four colour indices as a function of phase (1501 measurements for 256 O-rich Miras). The curves are the running average values and the arrows indicate the extreme values

colour diagrams. The filled circles mark phase zero and the arrows indicate the direction of variation during the cycle.

In the 78−88/105−104 diagram (Fig. 2), a loop is clearly described during the cycle. To a single 78−88 value two different 105−104 values corresponds, depending on whether the Mira is rising or declining. This loop confirms that a phase lag exists between 78−88 and 105−104. On the other hand, there is no loop in the 78−87/87−104 diagram (Fig. 3). It demonstrates the absence of phase shift and thus the occurence of extremes at more or less the same phase, as can be seen in Fig. 1. Similarly there is no phase lag between 78−88 and 78−87. Only 105−104 is out-of-phase by an amount of 0.1.

The presence (absence) of loop in the 78−88/105−104 (78−87/87−104) diagram is also verified when only a part of the sample of Miras is considered. Early and late spectral type Miras or short and long period sub-samples have been tried. The apparent phase shift and the presence of a loop in a colour-colour diagram which is its counterpart are independent of period and spectral type. The loop for shorter periods (higher $T_{\rm eff}$) is at smaller colour indices than that for longer periods (lower $T_{\rm eff}$).

3.3. Individual phase shifts

3.3.1. Method

The results described above concern only mean values. The trends revealed by this *global approach* should be verified by considering the individual sets of observations. In the following, we adopted the complementary *individual approach* to determine the possible phase shifts.

For each Mira with a number of observations at least equal to six (93 objects), we fitted the four indices as a function of phase φ by sine curves:

$$c_i = a_0 + a_1 \sin[2\pi(\varphi - \varphi_0)] \quad (1)$$

where c_i is one of the four colours; a_0, a_1 and φ_0 are the three free parameters.

We only used the Miras which have observed colours distributed in a phase range larger than 0.3 in order to properly fit the observations. We excluded the stars for which:

$$\max(c_i)_{\rm fit} > \max(c_i)_{\rm observed} + 0.4 \quad (2)$$

$$\min(c_i)_{\rm fit} < \min(c_i)_{\rm observed} - 0.4 \quad (3)$$

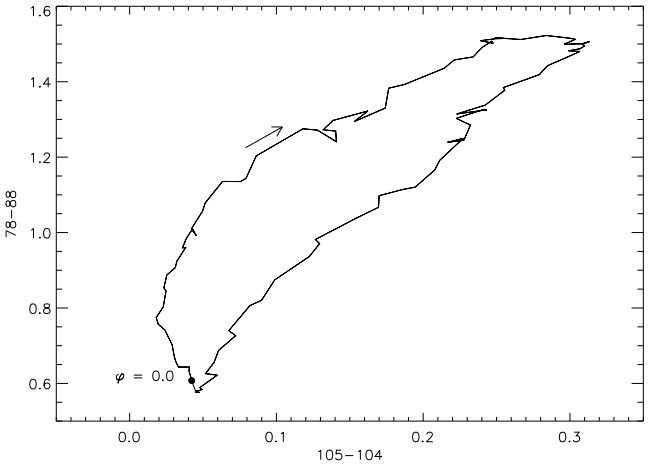

Fig. 2. 78−88/105−104 diagram. The curve represent the running average values shown in Fig. 1. The filled circle marks the phase zero and the arrow indicates the direction of variation during the cycle

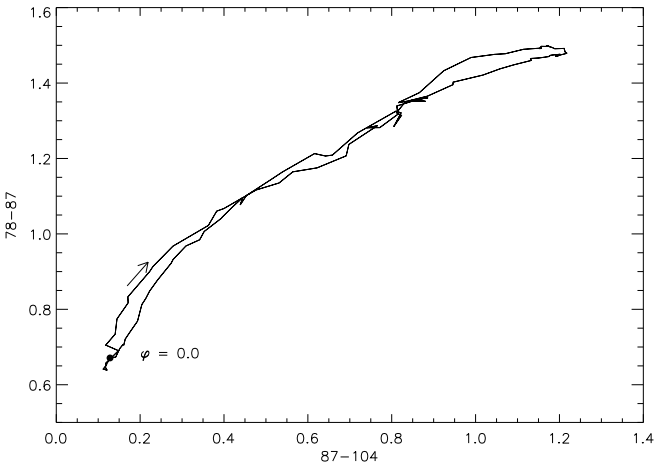

Fig. 3. Same as Fig. 2 for 78−87 and 87−104.

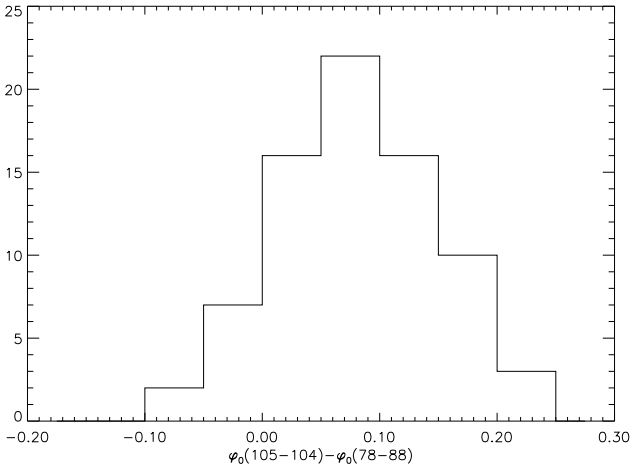

Fig. 4. Histogram of phase shifts: $\varphi_0(105-104)$ minus $\varphi_0(78-88)$

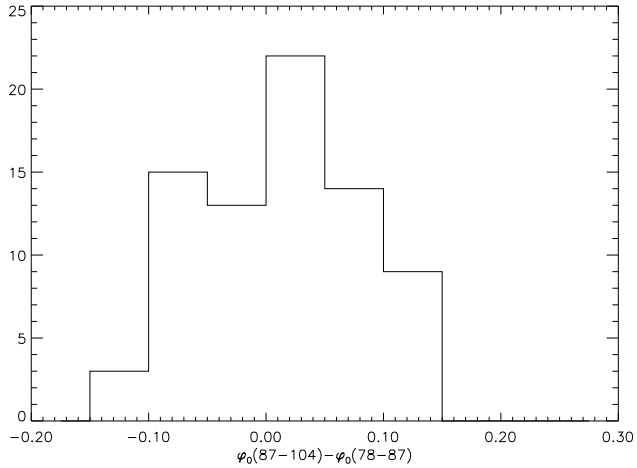

Fig. 5. Histogram of phase shifts: $\varphi_0(87-104)$ minus $\varphi_0(78-87)$

For these stars, the extremes given by the fit are too distant from the observations and thus are less reliable. Finally, we rejected the Miras with:

$$\max(105-104)_{\rm fit} < 0.05 \quad (4)$$

as it means that these stars show no appearance of VO absorption bands during the whole cycle (the temperature is always too high) and the fits have no meaning in these cases. There is no such problem with the other colours.

Among the 93 Miras with a number of observations greater than 5, 76 finally remained. The phase shift between two indices is simply:

$$\delta\varphi = \varphi_0(c_i) - \varphi_0(c_j) \quad (5)$$

3.3.2. Results

Fig. 4 presents the histogram of phase shifts between the (78−88, 105−104) indices. A majority of Miras clearly displays a phase lag. The distribution is almost symmetrical, the mean value being 0.08, with a sigma of 0.07. The variation of the 105−104 index lags behind that of 78−88, as it is observed in Fig. 1. The individual phase lag values are not correlated with period or spectral type. The histogram for the (78−87, 87−104) indices is shown in Fig. 5. No global phase lag is apparent as in Fig. 4. The calculated mean value is 0.01 with a sigma of 0.07.

The fit of the observations by sine curves is of course not really accurate and the individual phase lags determined with this method are not reliable, but both distributions provide an excellent statistical confirmation of what was concluded from the previous global approach: the 105−104 index appears out-of-phase with the other indices by an amount of almost 0.1, which corresponds to more or less 30 days for a typical Mira.

3.4. Comments on the phase lag

Lockwood (1972) already noted that Miras perform large loops in a colour/spectral-type diagram. He pointed out that the mean

phase of maximum light at 1.04 μm occurs at 0.11, whereas at V it occurs at phase zero by definition. Mean minimum light at 1.04 μm is reached almost simultaneously with mean minimum visual light, although the individual phases of these events often differ by 0.1 cycle or more.

We have shown that the phase lag and the loop phenomenon are also displayed by the particular near infrared indices considered here. More precisely, the phase shift is between the VO index on one hand and indices mainly related to TiO on the other hand. The phase lag between changes in the various bands which are dominated by different molecular absorption (TiO and VO) may be explained by the fact that these bands are formed at various depths in the atmosphere. What we see is a consequence of the shocks (created by the pulsation) running through the atmosphere.

Important progress in nonlinear stellar pulsation models has been made in the last years (Feuchtinger & Dorfi 1994, 1996a, 1996b; Bessell et al. 1996; Ya'ari & Tuchman 1996). Dynamical atmosphere models have also been successfully developed recently (e.g. Bowen 1988; Fleischer et al. 1992; Höfner & Dorfi 1997): the effects of pulsation generated in the interiors are simulated by periodic mechanical driving at the inner boundary (piston model). All these numerical simulations show that the propagation of successive shock fronts in the atmosphere creates a complex temperature, density, and velocity stratification. Parts of the atmosphere are heated up while others cool down. The run of temperature is often far from the smooth decrease found in static LTE models. As a consequence, during a fraction of the cycle, the VO molecular lines can still be building up strength, as e.g. VO molecules are forming (the VO index increases), while the TiO lines have started to weaken (TiO indices decrease): a loop then appears in the corresponding colour-colour diagram. We will try to investigate this hypothesis in Sect. 5 by using a set of dynamical atmosphere models to compute the colours variation during a cycle, but this requires that we are first able to well reproduce Lockwood's colours for non-variable M-giants. This is the aim of the following section.

4. M-giant standards and hydrostatic model colours

The first step in any attempt to investigate the origin of the phase lag is to correctly reproduce Lockwood's colours for M-giants. It is now possible thanks to important progress in the modelling of red giant atmospheres achieved in the last years (Plez et al. 1992, hereafter PBN92; see also the review by Plez 1997).

4.1. The synthetic spectrum program

We computed synthetic spectra with TurboSpectrum, an enhanced version of the Spectrum package developed at Uppsala observatory and used in previous investigations of AGB stars (e.g. Plez et al. 1993). Input model atmospheres were calculated with SOSMARCS (PBN92), one of the latest developments in the MARCS suite of programs initiated by Gustafsson et al. (1975). SOSMARCS generates spherically symmetric, hydrostatic, flux constant (convective + radiative) models in LTE. It is especially designed for cool star atmospheric conditions. It features a full Opacity Sampling treatment of all opacities with 10912 sampling points between 990 and 125000 Å. TurboSpectrum is based for a large part on the same ensemble of routines (e.g. evaluation of continuous opacities and solution of the transfer equations). Any kind of temperature-pressure stratification may be used and the execution time is relatively short even when millions of lines are taken into account. It offers the possibility for instance to test complex profiles which can mimic pulsating atmospheres, and perform extensive calculations with various abundances and/or line lists.

4.2. The atomic and molecular data

We included for the spectrum computations atomic line data from N to Ni (Kurucz 1992). We also included line lists for the TiO α, β, γ, γ', δ, ϵ, ϕ and a-f electronic transition systems, the VO A-X and B-X electronic transition systems, and a newly calculated line list for H_2O (Jørgensen, private communication). The absorption systems of $^{12}C^{14}N$ and $^{13}C^{14}N$ (Jørgensen & Larsson 1990) are also taken into account, with a $^{12}C/^{13}C$ ratio equal to 19, which is a typical value after the first dredge-up (Smith 1990).

Most of the TiO and VO band strengths were updated since PBN92. In PBN92 the electronic transition momenta (R_e^2) of Davis et al. (1986) were adopted for the TiO α, β, γ, γ', δ and ϕ systems, supplemented by Brett's astrophysical calibration for the TiO ϵ (Brett 1990). In subsequent works (e.g. Plez et al. 1993) the lifetime measurements of Doverstål & Weijnitz (1992) replaced some of the earlier values. Recently Hedgecock and coworkers (1995) performed lifetime measurements with a better accuracy and for a larger number of electronic states than previously for the α, β, γ and γ' systems. These new lifetime values are significantly different from the older ones. We decided to adopt them in our investigation. We generated also a line list for the a-f system using the lifetime given by Hedgecock et al. (1995, experimental), and Schamps et al. (1992, theoretical) which agree within 5%. This system absorbs mostly in the V band region and has no impact on the present calculations. For the TiO ϕ (Hedgecock et al. did not measure the corresponding lifetime) and the ϵ (the same authors provide only an upper limit of the strength) systems, the results of the recent ab initio calculations performed by Langhoff (1997) are adopted. His calculations for the other bands are in good agreement with the Hedgecock et al. values. We included all 5 stable isotopes of Ti with terrestrial abundance ratios in the computation of the line list.

The VO A-X and B-X band strengths in PBN92 result from the astrophysical calibration by Brett (1990) and are not expected to be very reliable especially as they were calibrated using outdated mean opacity models. Recently, Karlsson et al. (1997) measured the lifetimes of the A, B and C electronic states. We included their values in our line list which was also revised using Cheung et al. (1982a, 1982b, 1994), and Adam et al. (1995). The new line positions are shifted by up to 65 cm^{-1} (-40 Å) in the B-X system, and 25 cm^{-1} in the A-X system

Table 2. Adopted electronic transition momenta for the TiO systems

System	$R^2_{\rm e,Davis}$	$R^2_{\rm e,this\ work}$	resulting $f_{\rm e}$-value	$\frac{R^2_{\rm e,this\ work}}{R^2_{\rm e,Davis}}$
α	3.0	1.8[a]	0.106	0.6
β	5.14	2.3[a]	0.125	0.45
γ	3.6	1.84[a]	0.0786	0.51
γ'	2.8	1.9[a]	0.0935	0.68
δ	1.4	1.4	0.048	1.0
ϵ	–	0.064[b]	0.0023	–
ϕ	0.9	0.32 [b]	0.0178	0.36
a-f	–	1.69[a]	0.098	–

[a] based on lifetime measurements (Hedgecock et al. 1995)
[b] based on lifetime calculations (Langhoff 1997)

Table 3. Adopted electronic transition momenta for the VO systems

System	$R^2_{\rm e,Brett}$ [a]	$R^2_{\rm e,this\ work}$ [b]
A-X	0.207	0.106
B-X	2.590	0.735

[a] astrophysical calibration by Brett (1990)
[b] based on lifetime measurements (Karlsson et al. 1997)

compared to PBN92. The line-strengths are scaled by a factor 0.51, 0.28, and 0.72 for the A-X, B-X, respective C-X transitions relative to PBN92's values.

We summarize the $R^2_{\rm e}$ and the electronic oscillator strength ($f_{\rm e}$-values) we used in Table 2 and 3 for the TiO and VO systems respectively. Like Larsson (1983), we prefer to avoid the discussion of $f_{\rm e}$-values which lack a sound and unique definition in molecular spectra. We provide them anyway as a guide for comparison with other works (e.g. Jørgensen 1994). We define $f_{\rm e}$ through: $f_{\rm e} = 3.038 \times 10^{-6} \times \overline{\sigma}_{00} \times R^2_{\rm e} \times \frac{2-\delta_{0,\Lambda'+\Lambda''}}{2-\delta_{0,\Lambda''}}$, where $\overline{\sigma}_{00}$ is some average wavenumber for the (0-0) band of the transition system, $'$ and $''$ denote the upper and lower state respectively, and Λ is the projection of the electron orbital angular momentum (0 for Σ states, 1 for Π states etc); see Larsson for more details.

As shown in Table 2 and 3, almost all TiO and VO band strengths have been obtained from recent laboratory measurements or calculations. Apart from the δ system, all bands have been updated since PBN92. The choice to keep the Davis et al. value for the δ system comes from comparisons between observed and calculated spectra for a sample of M giants and dwarfs. Adopting Langhoff's lifetime for $b^1\Pi$ and branching ratios for the δ and ϕ transitions leads to obviously too strong δ bands. We could not find an explanation for this mismatch and decided therefore to keep the seemingly better value from Davis et al. (1986), which also matches Ramsey's (1981) measurements of the δ(0-0) bandhead at 8160 Å rather well down to $T_{\rm eff} \sim 3400$ K. Adopting Langhoff's value, which is twice as large, results in a calculated Ramsey's D_{8860} index systematically too large by 0.1 to 0.14. This is however puzzling and will be further investigated by Plez et al. (in preparation) in their discussion of the new large grid of Uppsala models.

Davis et al. (1986) used the lifetime of the upper state of a transition in the β system measured by Feinberg & Davis (1977) to put their measurement of relative transition momenta on an absolute scale. Our revision of the β system strength, following Hedgecock et al. lifetime measurement, amounts to a downward scaling by a factor 0.45 of Davis et al. value. For the other bands quoted by Davis et al. the factor is between 0.36 and 0.68 (see Table 2).

Table 4. Dominant molecular features in each band of Lockwood's photometric system

Filter	Dominant systems	Less influent systems
78	TiO γ	VO B-X, TiO γ', δ and ϵ
87	TiO γ and VO B-X	TiO ϵ
88	TiO δ, γ and VO B-X	TiO ϵ and VO A-X
104	–	TiO ϕ, δ, ϵ and γ
105	VO A-X	TiO ϵ, γ, ϕ

4.3. Influence of the various molecular bands on colours

We first computed individual spectra for each absorption band system in order to establish its particular influence on Lockwood's passbands. Table 4 presents the systems which are really dominant in each band and those for which the influence is less pronounced but still measurable. The systems that are not listed have no significant influence.

The most prominent features measured by the filters are the TiO γ and δ systems, and the VO A-X and B-X systems. A noticeable result is the relatively important influence of VO absorption on the 87 and 88 filters. Furthermore, when the $T_{\rm eff}$ reaches values lower than 2800 K, the features due to the VO B-X system become even stronger than those due to TiO bands in our models. This effect was not expected by Lockwood. Concerning the continuum points, the 104 filter can effectively be considered as a good measurement of a region relatively free of strong molecular absorption; this is certainly not the case for the 87 filter. The CN and H_2O bands and the atomic lines have no significant effect on the emergent fluxes in the filter passbands.

The Lockwood colours, as they measure the influence of a limited number of molecular band systems as shown in Table 4, constitute an ideal opportunity to check the calibration of some of those TiO and VO bands and/or the accuracy of the models and the synthetic spectra.

4.4. Comparison to observations

Lockwood has observed 61 standard red giants with spectral types from K5 to M8 in the same five-colour system as the Mira variables. In order to compare these observations with synthetic colours, we used fifteen SOSMARCS models representing a sequence of red giants with solar composition, a stellar mass of

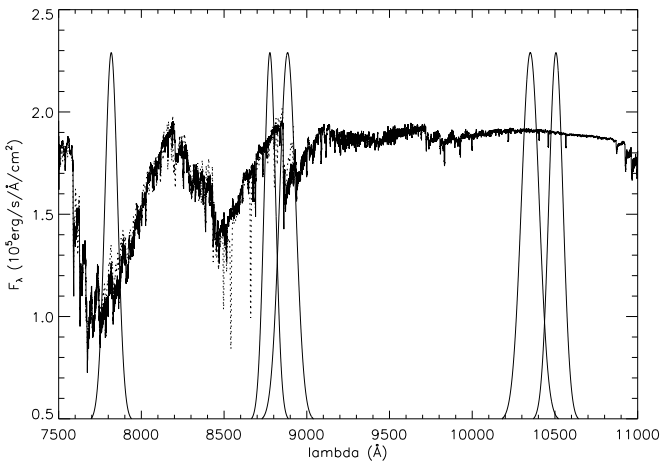

Fig. 6. Synthetic spectrum with $T_{\rm eff}$ = 3500 K, log g=0.9, $\mathscr{M}$=1.5 $\mathscr{M}_\odot$. The dotted line is part of an optical spectrum of HD 123657, a M5-giant, from Serote Roos et al. (1996). The CaII triplet lines are not included in the synthetic spectrum. The filter transmission curves used in this work are superimposed (full line)

1.5 $\mathscr{M}_\odot$ and $T_{\rm eff}$ ranging from 2500 to 3900 K. The surface-gravities log g vary from 1.60 at $T_{\rm eff}$ = 3900 K to -0.50 at $T_{\rm eff}$ = 2500 K. These models were used by Fluks et al. (1994) and are further described there. The emergent fluxes were computed between 7500 and 11000 Å with a resolution of 0.2 Å. Changing the sampling to 0.8 Å changes the colours by at most a few hundredth of a magnitude. Fig. 6 shows an example of a synthetic spectrum ($T_{\rm eff}$ = 3500 K). The dotted line is part of an optical spectrum of HD 123657 (BY Boo), a M5-giant, obtained by Serote Roos et al. (1996) at a resolution of 1.25 Å using the Aurelie spectrograph, attached to the OHP 1.52m telescope. The region covered ends at 8920 Å. The agreement is very good.

Lockwood's filters of Table 1 were applied to the fifteen spectra. The zero point calibration is based on a spectrum of Vega (Dreiling & Bell 1980) as used by Bessell & Brett (1988). An effective temperature has been assigned to each standard giant using the spectral types given in L72, and the spectral type-$T_{\rm eff}$ relation determined by Fluks et al. (1994). The overall good agreement of the synthetic and observed colours is demonstrated in Fig. 7.

A small but systematic discrepancy exists for the 78−88 and 78−87 indices when they are greater than 0.8 (Fig. 7a and b). Furthermore, both colours are not ever-increasing along the sequence of $T_{\rm eff}$. The observed variation with phase of these indices in the Miras sample brings the conclusion that this behaviour is apparently not real. The synthetic 87−104 colours are maybe also slightly above the observed ones for temperatures lower than 3300 K (Fig. 7c). The 105−104 index appears to be the least well-modelled (Fig. 7d), but note that its scale of variation is a factor 10 smaller than the other colours.

Discrepancies might be due to uncertainties in the:

– narrow-band filter shapes (a gaussian shape was assumed) and in the zero point calibration: this may imply a systematic error. It seems this is the case at least for the 105 filter (see Fig. 7d). Standard errors quoted by Lockwood for 104 are ±0.012 mag. Errors in our zero points are probably of the same order of magnitude. This is problematic only for 105−104, which has a very small range of variation.
– spectral types attributed by Lockwood: some stars have the same spectral type whereas they exhibit rather distinct colours. Furthermore, the scale of spectral subtypes (M0 to M10) adopted by Fluks et al. for their SpT-$T_{\rm eff}$ relation might differ from the one used by Lockwood.
– laboratory measurements and calculations of lifetime as quoted by the different authors: the uncertainties are still important despite great progress made recently in the TiO and VO bands calibration.

Furthermore, red giants naturally exhibit a spread of effective temperature, but also of stellar masses, gravities and chemical composition. Fig. 7 shows only a 'one-dimensional' fit (in $T_{\rm eff}$): $\mathscr{M}$ and log g have a non-negligible effect on colours and part of the discrepancy might also be explained by this. Test calculations using models taken from the grid of Plez (1992) show that two models with the same $T_{\rm eff}$ and luminosity but with distinct log g and $\mathscr{M}$ have differences of tenths of mag for some indices (e.g. at 3000 K, the log g=−0.7 and $\mathscr{M}$=1 model differs by −0.06 in 78−87, −0.007 in 78−88, 0.37 in 87−104, and 0.042 in 105−104 from the log g=0.00 and $\mathscr{M}$=5 model). We recall that the sequence of models was computed using the Ridgway et al. (1980) temperature calibration, and a theoretical red-giant branch from Lattanzio (1991) to relate the effective temperature and luminosity, assuming a mass of 1.5 $\mathscr{M}_\odot$.

The effect of relative abundance changes in C and N was also checked. Some spectra were recomputed with a change of −0.2 dex in the C abundance and +0.5 dex in the N abundance, which are typical values after dredge-up (Smith 1990). The difference is less than a tenth of a magnitude in all colours at 3100K, and largest for 87−104.

The fit for the 105−104 index is not excellent below $T_{\rm eff}$ $\sim$ 3100 K. However, the variation scale is less than 0.2 mag. Uncertainties in the observations are of the order of 0.006 mag for the colours, according to Lockwood. We suspect the flux level of our models around 1μm to be slightly too high. This appears also when comparing them to observed spectra of M-giants. There may be a missing opacity in our computations. This will be further investigated by Plez et al. (in preparation). Note also that the points at $T_{\rm eff}$ $\leq$ 3100 K consist of X Her, EP Aqr, BK Vir, RT Vir, SW Vir and RX Boo, which are all variables. In conclusion, keeping in mind the above discussion, the agreement between the synthetic and observed colours is remarkable in Fig. 7, and provides a quite safe basis for the study of Miras.

5. Miras and hydrodynamical model colours

Now that we are confident about the line lists and our synthetic colour calculations we may try to compute them for Mira stars. An examination of Fig. 1 readily shows that the variation of the 87−104 and 105−104 colours for Miras greatly exceeds the

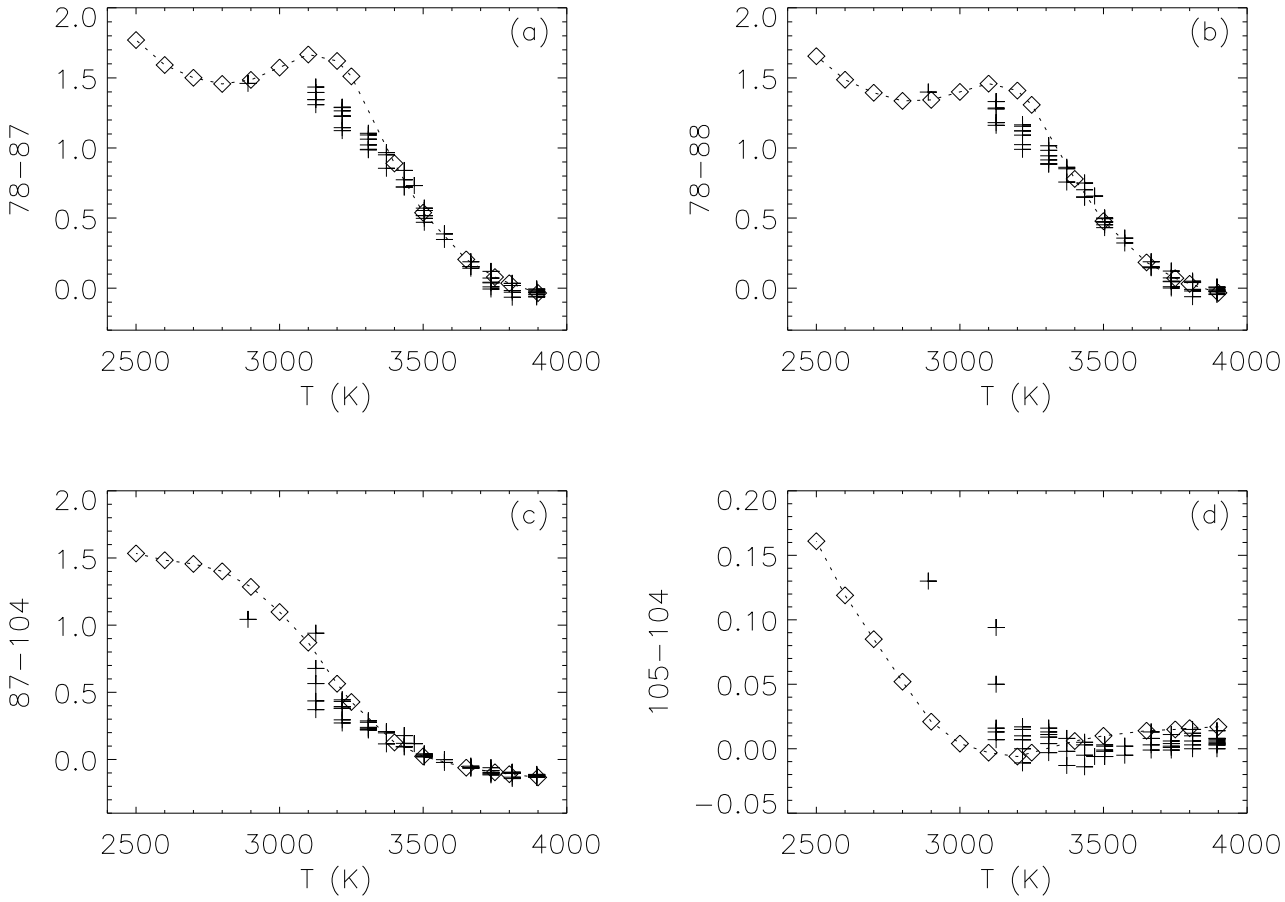

Fig. 7a–d. Comparison of synthetic and observed indices in temperature-colour diagrams. Crosses are the red giants observed by Lockwood. Diamonds represent the sequence of hydrostatic models with $T_{\rm eff}$ ranging from 2500 to 3900 K

range of static models, whereas this is not the case for 78−87 and 78−88. Together with the phase lag between 105−104 and the other colours, this shows that static models will not be able to reproduce the colour variations along the cycle of Mira stars.

S. Höfner (1997) kindly provided us with a sequence of models (50 in total distributed on 2 successive cycles) with the parameters: $\mathscr{M}_\star$ =1 $\mathscr{M}_\odot$, $L_\star$ = 7000 $L_\odot$, $T_\star$ = 2880 K, P = 390 d, and a piston velocity of 4 km.s^{-1}. This model was already used by Loidl et al. (1997) to synthetize C-rich IR spectra and is similar to the models presented by Höfner & Dorfi (1997) except for the gas opacity which was adjusted by comparison with standard model atmospheres to give more realistic gas densities. It was computed with C/O=1.8, which is not adapted to our O-rich objects. However, there are no suitable O-rich hydrodynamical models available, and we only want to qualitatively understand the phase lag. A likely explanation is that this phase lag arises from the difference in formation depth of the various spectral regions dominated by continuum, TiO or VO bands, combined with the running temperature T- and density ρ- perturbations along a cycle. For the purpose of this work we may assume that the chemistry used in the computation of the hydrodynamic model is not a key issue (especially as it is hardly reflected in the radiative transfer, treated in the grey case with a constant opacity of 10^{-2} cm^2.g^{-1}; the C-rich chemistry has however a strong impact on the dust formation). We therefore only used the T and ρ stratification of the models in R, recomputed the chemical equilibrium with a solar composition, to derive the electronic pressure $P_{\rm e}$ and an optical depth scale τ. We did not use all the 500 points of the original models but selected about 65 depth-points with an average separation of 0.2 in $\Delta \log \tau$, which is sufficient for treating the radiative transfer. We slightly extrapolated the models inwards to increase the maximum τ value in order to provide a better inner boundary condition (diffusion approximation), but the exact stratification deep in the model has no strong impact on the emergent spectrum.

As noted above, we surmise that the phase lag is due to a difference in the depth of formation of VO bands (dominating at 105) and TiO bands. A first and quick qualitative check is offered by the variation in column density of TiO and VO along a pulsation cycle of the model. The column densities are obtained by calculating the chemical equilibrium at each depth point of the dynamical models and integrating the number densities radially. The column densities oscillate up and down along the cycle (Fig. 8). The phase lag is 0.065 at minimum column density and 0.030 at maximum, the VO variation lagging behind

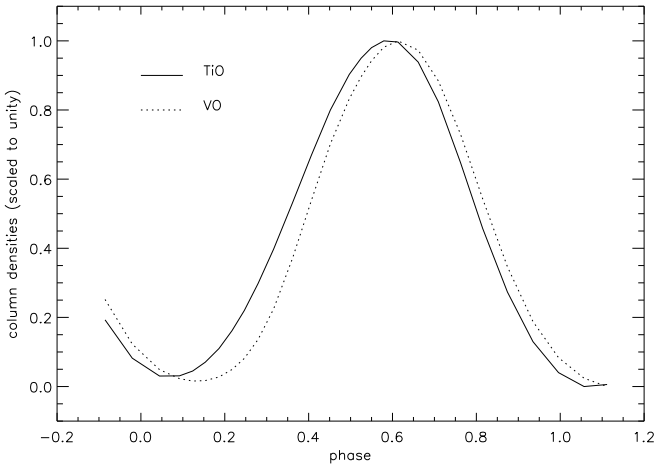

Fig. 8. TiO and VO column densities as a function of phase, computed assuming chemical equilibrium in the hydrodynamical model of Höfner. Both column density variations have been scaled to the [0 ; 1] interval to facilitate comparison. The column densities vary between $3.9\,10^{17}$ and $1.6\,10^{18}$ g.cm^{-2} for TiO, and $5.2\,10^{15}$ and $5.0\,10^{16}$ g.cm^{-2} for VO

TiO's, providing a first qualitative confirmation of our hypothesis. The ratio of the column densities is about 50, a factor 5 larger than the abundance ratio of Ti and V.

We also computed LTE synthetic spectra for these models in the same fashion as for static models. The velocity fields were neglected. The resulting colours are displayed in Fig. 9. To facilitate the comparison with observations we have also plotted in this figure the mean relation from Fig. 1 for each colour. We have allowed for 2 shifts of the observed colours, relative to the observations. The first shift, identical for all 4 colours, is in phase (the calculated curves are shifted by 0.08). There are no *a priori* reasons for the zero of the phase to be the same in the observations and in the models. For the observations, we recall that the zero is defined as the maximum light in V band. In the models, the zero is defined as the time when the piston moves outwards with its maximum velocity. We also shifted the data vertically to allow an easier comparison of the shape and amplitude of the curves. The scale on the right-hand side of the diagrams is for the observed data, the one on the left-hand side is for the synthetic colours. The agreement is surprisingly good.

The minima are all reasonably well matched with the possible exception of the 87−104 index. From the calculated minima we find a phase lag of 0.09 of 105−104 relative to 78−87 and 78−88 in very good agreement with the value derived from observations (0.08). We also find a slight phase lag for 87−104 of 0.04, which is also detectable in the observations at minimum light, and due to the hybrid nature of this index. The maxima are more discrepant, especially for 78−87 and 78−88, with a tendency for the synthetic colours to show a secondary minimum. We suspect this to be due to the same cause as the S-shape shown in Fig. 7 by the synthetic colours of static models around 3000 K; we believe this S-shape to be in error. It is possible that additional absorbers missing in our synthetic spectra would solve the discrepancy. A more serious problem is that the 78−87 and 78−88 synthetic indices are 1.5 to 2 mag too large in absolute value, although their amplitude of variation is about right. As 87−104 is of the right magnitude, it could be that this problem stems from an inadequate value of the 78 flux. A more detailed discussion is not useful given the approximations we have made. We have used *one* specific *C-rich* hydrodynamical model stratification for which we have computed an *LTE* radiation transfer with an *O-rich* equilibrium chemistry. We have compared the result of these calculations for a unique set of model parameters to *mean* colour variations resulting from the average of 256 different Mira stars. It is actually amazing that we get such a good agreement. But one should certainly perform the same computations for a series of models with various $\mathscr{M}_\star$, $L_\star$, P, $\dot{\mathscr{M}}$, and check for possible variations of the phase lag, of the amplitude of variations of the various indices, etc. It would also be desirable to use O-rich models. One more limitation of our approach is that we have neglected the velocity field that shifts spectral lines differentially with depth. In this particular model the velocity of the gas is of the order of +15 to -15 km.s^{-1} in the line formation zone. This will spread out the opacity, block more flux between the lines and allow more photons to escape within the lines. This may solve some of the discrepancies we discussed above.

6. Conclusions

Using Lockwood's (1972) five-colours observations of 256 O-rich Miras we found evidence for the loops described by these stars in colour-colour diagrams, and a phase lag between the VO and TiO indices, reflecting the shocks running through the extended stellar atmosphere. We used the best current hydrostatic and hydrodynamic model atmospheres, and line lists to compute synthetic colours for normal M-giants and Miras. We found that the normal M-giant colours are rather well reproduced, at least for $T_{\rm eff}$ above 3100 K. Missing opacity sources, non-LTE, non-thermal heating, variability may all explain the worse match to observations at later spectral-types. This is worth further study, but for earlier spectral-types model atmospheres and synthetic spectra are reaching a high quantitative agreement with observations. This is very encouraging for the next (and last) generation of classical models in preparation in Uppsala that will include even more up-to-date and more complete opacities (Plez et al. in preparation).

Our experiments in solving LTE radiative transfer in one series of hydrodynamical models (Höfner, private communication) have worked beyond our expectations. We found approximately the right variation of the colours and the right phase lag between them. The fit is of course not perfect, and should not be. We used one specific model and the observations are an average of 256 different stars. There are many more limitations in the modelling (e.g. LTE, no account of velocity field, ...), but the main point is that hydrodynamical models, equilibrium chemistry, and LTE radiative transfer seem to reproduce at least some of the observed data on Miras (cf. also the work of Loidl et al. 1997 on IR spectra of C-rich Miras). This may be surprising

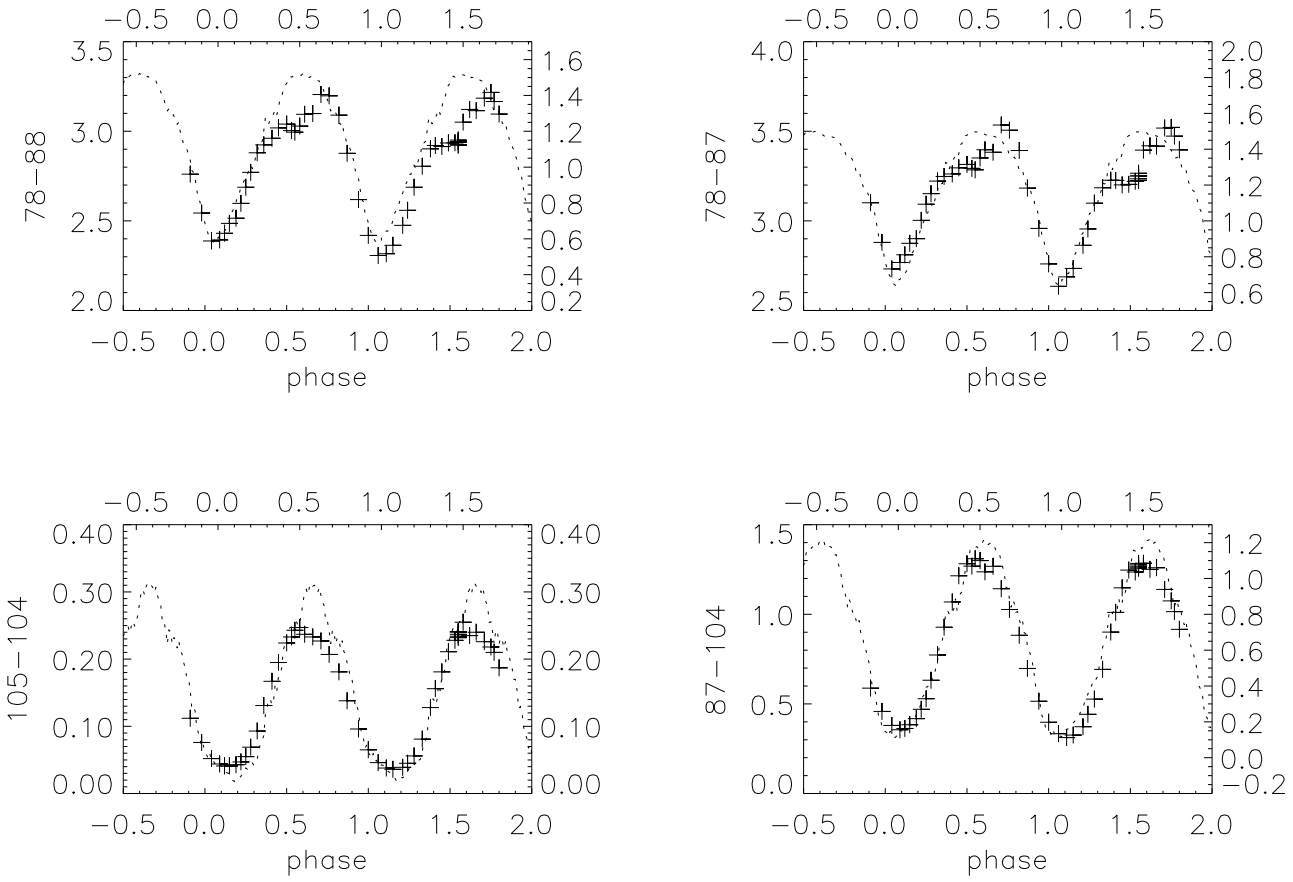

Fig. 9. Comparison of synthetic colours of dynamic models (crosses; left-hand side and bottom scales) and observed mean relations from Fig. 1 (dotted curves; right-hand side and top scales)

at first sight. We cannot just assume that equilibrium and LTE prevail all through Miras atmospheres. This has to be checked, and that is a heavy task. The advantage of the present approach is that it allows us to account for millions of spectral lines, carry a large number of tests (vary chemical composition, ...) while keeping the computation time into reasonable bounds. We could easily compute center-to-limb intensity profiles as well. We believe this work opens the prospect of calculating accurate colours and spectra for cool stars, not least long-period variables (LPV's). The out-of-phase variations of the various spectral features, reflecting the propagation of perturbations (shocks) in the atmospheres are a very strong constraint to the models. The confrontation to spectrophotometric observations, resolving the absorption bands, along the whole cycle, will be necessary to test the models and better understand LPV's atmospheres, pulsation and mass-loss. It will also unveil limitations/inadequacies in the hypotheses made in the modelling. This would be a very useful program for a small telescope equiped with an $R \approx 10\,000$ spectrograph, ideally reaching wavelengths up to 1.1 micron.

Acknowledgements. S. Höfner and her collaborators are warmly thanked for providing us with extensive data from one of their hydrodynamical model and for useful discussions and suggestions. S. Langhoff is acknowledged for sending us the result of his TiO calculations prior to publication. We thank U.G. Jørgensen for financial support while RA was staying at the Niels Bohr Institute. Part of this work was carried out while BP held a fellowship from the EU HCM program at NBI. BP thanks the GRAAL for a most pleasant stay during the final stage of this work.

References

Adam A.G., Barnes M., Berno B., Bower R.D., Merer A.J., 1995, J. Molec. Spectrosc. 170, 94
Alvarez R., Mennessier M-O., 1997, A&A 317, 761
Bessell M.S., Brett J.M., 1988, PASP 100, 1143
Bessell M.S., Scholz M., Wood P.R., 1996, A&A 307, 481
Brett J.M., 1990, A&A 231, 440
Bowen G.H., 1988, ApJ 329, 299
Cheung S.C., Hansen R.C., Merer A.J., 1982a, J. Molec. Spectrosc. 91, 165
Cheung S.C., Taylor A.W., Merer A.J., 1982b, J. Molec. Spectrosc. 92, 391
Cheung S.C., Hajigeorgiou P.G., Huang G., Huang S.Z., Merer A.J., 1994, J. Molec. Spectrosc. 163, 443
Davis S.P., Littleton J.E., Phillips J.G., 1986, ApJ 309, 449
Doverstål M., Weijnitz P., 1992, Molec. Physics 75, 1375
Dreiling L.A., Bell R.A., 1980, ApJ 241, 736
Feinberg J., Davis S.P., 1977, J. Molec. Spectrosc. 69, 445
Feuchtinger M.U., Dorfi E.A., 1994, A&A 291, 209
Feuchtinger M.U., Dorfi E.A., 1996a, A&A 306, 837

Feuchtinger M.U., Dorfi E.A., 1996b, A&A in press
Fleischer A.J., Gauger A., Sedlmayr E., 1992, A&A 266, 321
Fluks M.A., Plez B., Thé P.S. et al., 1994, A&AS 105, 311
Gustafsson B., Bell R.A., Eriksson K., Nordlund Å., 1975, A&A 42, 407
Hedgecock I.M., Naulin C., Costes M., 1995, A&A 304, 667
Höfner S., Dorfi E.A., 1997, A&A 319, 648
Jørgensen U.G., 1994, A&A 284, 179
Jørgensen U.G., Larsson M., 1990, A&A 238, 424
Karlsson L., Lindgren B., Lundevall C., Sassenberg U., 1997, J. Molec. Spectrosc. 181, 274
Kholopov P.N. (ed.), 1985, 1987, General Catalogue of Variable Stars, Fourth Edition, Nauka Publ. House, Moscow
Kurucz R.L., 1992, Rev. Mex. Astron. Astrofis. 23, 45
Langhoff S.R., 1997, ApJ 481, 1007
Larsson M., 1983, A&A 128, 291
Lattanzio J.C., 1991, ApJS 76, 215
Lockwood G.W., 1972, ApJS 24, 375 (L72)
Loidl R., Hron J., Höfner S. et al., 1997, ApSS in press
Plez B., 1992, A&AS 94, 527
Plez B., 1997, In: R.F. Wing (ed.) The Carbon Star Phenomenon, in press
Plez B., Brett J.M., Nordlund Å., 1992, A&A 256, 551 (PBN92)
Plez B., Smith V.V., Lambert D.L., 1993, ApJ 418, 812
Ramsey L.W., 1981 AJ 86, 557
Ridgway S.T., Joyce R.R., White N.M., Wing R.F., 1980, ApJ 235, 126
Schamps J., Sennesal J.M., Carette P., 1992, J. Quant. Spectrosc. Rad. Transfer 48, 147
Serote Roos M., Boisson C., Joly M., 1996 A&AS 117, 93
Smith V.V., 1990, Mem. Soc. Astron. Ital. 61, 787
Wing R.F., 1967, In: M. Hack (ed.) Colloquium on late-type stars, Osservatorio Astronomico di Trieste, p.231
Ya'ari A., Tuchman Y., 1996, ApJ 456, 350

This article was processed by the author using Springer-Verlag LaTeX A&A style file *L-AA* version 3.